Stability Analysis of Grid for Variation in the System Performance

N.Sreeramulu reddy, M.Pala prasad reddy, V.Ishaku

Abstract— **Microgrid is an aggregation of distributed generators (DGs) and energy storage systems (ESS) through corresponding power interface, such as synchronous generators, asynchronous generators and power electronic devices. Without the support from the public grid, the control and management of an autonomous microgrid is more complex due to its poor equivalent system inertia. To investigate microgrid dynamic stability, a small -signal model of a typical microgrid containing asynchronous gener-ator based wind turbine, synchronous diesel generator, power electronic based energy storage and power network is proposed in this paper. The small-signal model of each of the subsystem is established respectively and then the global model is set up in a global reference axil frame. Eigenvalues distributions of the microgrid system under certain steady operating status are identified to indicate the damping of the oscillatory terms and its effect on system stability margin. Eigenvalues loci analysis is also presented which helps identifying the relationship among the dynamic stability, system configuration and operation status, such as the variation of intermittent generations and ESS with different control strategies. The results obtained from the model and eigenvalues analysis are verified through simulations and experiments on a study microgrid system.**

Index Terms—**Distributed generators, dynamic stability, energy storage system, microgrid, small-signal model.**

I. INTRODUCTION

Microgrid can be considered as an advanced organi-zation of distributed generation systems with less infl u-ence from the stochastic distributed generations (DGs), such as PV arrays and wind turbines, through proper control of energy storage systems (ESS) and dispatched loads [1], [2].

Microgrid plays important roles in the effective utilization of renewable energies and the stable operation of the public power grid [3], [4]. It makes the massive development of the renewable ener-gies possible.

Normally, DGs can be connected into microgrid through power electronic converters or rotating machines [5]. The former responds rapidly to the power control and make mi-crogrid operation more flexible; however, they are potentially susceptible to the oscillation under system disturbances [6].

While the latter usually involves synchronous generators

N.Sreeramulu reddy, Assistant Professor, Department of Electrical & Electronics Engineering,Annamacharya Institute of Technology & Science, Rajampet, Andhra pradesh, INDIA

M.Pala prasad reddy, Assistant Professor, Department of Electrical & Electronics Engineering,Annamacharya Institute of Technology & Science, Rajampet, Andhra pradesh, INDIA

V.Ishaku, PG Student, Department of Electrical & Electronics Engineering,Annamacharya Institute of Technology & Science, Rajampet, Andhra pradesh, INDIA

equipped with excitation and governor systems, and asyn-chronous wind turbine (AWT) of small or medium capacity.

While the latter usually involves synchronous generators equipped with excitation and governor systems, and asyn-chronous wind turbine (AWT) of small or medium capacity.

A typical microgrid usually has two kinds of operation modes, *i.e.*, autonomous operation mode and grid -connected operation mode. To guarantee the reliable power supply for essential loads, the smooth transition between these two modes is usually required [7], [8]. Without the support from the main grid, the control and management of the autonomous operation microgrid is often more complex than the grid-connected one. Since the equivalent physical inertia of microgrid is quite smaller compared with the main grid [4], some medium or even small interruptions such as the output power fluctuation of PV arrays or wind turbines, and the cut in or cut off of local loads may result in power quality and stability issues. Specifically, the frequency and voltage quality would decline, and system stability would deteriorate.

With the development of power electronics, energy storage can be controlled to release or absorb active/reactive power flexibly. When ESS is integrated into microgrid, it can main-tain system instantaneous power balance and improve the dy-namic performance through proper energy management strate-gies, which equals to system equivalent inertia enhancement [9]. Therefore, the impact of DGs' power fluctuations and other in-terruptions on system stability and power quality can be miti-gated greatly, which is of vital importance for microgrid in au-tonomous operation mode. Many energy storage technologies and their applications in microgrids were studied recently in-cluding Li-ion batteries, flywheel energy storage (FES), super-capacitors, superconducting magnetic energy storage (SMES) and vanadium redox battery (VRB), etc. [10], [11].

One of the important concerns in the reliable operation of mi-crogrid is small-signal stability [8]. In conventional power sys-tems, stability analysis is well established with standard models of synchronous machines, governors and excitation systems of varying orders that are known to capture the important modes for particular classes of problems. This does not yet exist for microgrids and may be hard to achieve because of the wide range of power technologies that might be deployed. Therefore, full- order models of microgrids with typical DGs are required. The small-signal models containing synchronous generators, in-verter based generations and power network were established in [5] and [12], and the dynamic characteristics in autonomous operation mode were analyzed based on the individual models. The global

small-signal model of the inverter based microgrid was setup in [8] to design the controller of inverter based DGs. However, as an important DG, asynchronous wind turbine was not included in the model.

In this paper, a small- signal model of a typical microgrid is presented. It will contain the major types of power interface de-
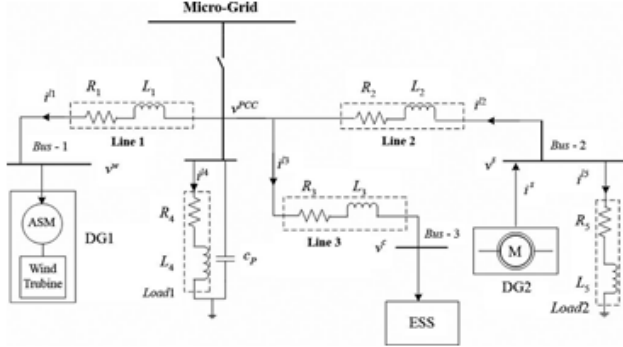

Fig. 1. Single-line diagram of a typical microgrid.

vices of DGs exist nowadays such as synchronous generator, asynchronous generator and inverter. Each of the small-signal models of the individual DGs will be established respectively together with that of the power network, and then the global model will be set up in a global reference axil frame. Once the small -signal model has been constructed, eigenvalues are iden-tified to indicate the damping of the oscillatory terms under dif-ferent operation conditions. The analytical nature of this exam-ination then allows further investigation of the relation between stability and system configurations, such as DGs capacity and system operating state. A sensitivity analysis is then conducted by tracking eigenvalues loci under certain conditions, which provides the difference between the situations with/without ESS on system stability. The theoretical analysis is verified with both simulations and experiments of a typical microgrid.

The rest of the paper is organized as follow. Section II de-scribes the mathematical model of a typical microgrid system. Section III analyzes the small -signal dynamic stability by eigen-values loci tracking. Results and discussions of the simulation and experiment are reported in Section IV. Conclusion is stated in Section V.

II. MATHEMATIC MODEL OF MICROGRID

Fig. 1 shows the single-line diagram of a typical microgrid. It comprises, instead of local loads, DG1 representing an AWT with stall regulation, DG2 representing a synchronous gener-ator equipped with excitation and governor control systems, and an ESS based on a voltage-sourced converter (VSC) with ac-tive/reactive power controller. It is connected to a distribution network at the point of common coupling (PCC), and operates autonomously when the main grid is fault.

The state-space model of DG1, DG2, ESS and power net-work are represented on their individual local reference frame, respectively. A common reference frame is chosen as the global reference frame of the microgrid system, and all of the subsys-tems are shift to the global reference frame using

the transfor-mation method shown in Fig. 2 and formulated in (1)[13].

As shown in Fig. 2, the d-axis and q-axis is taken as the global reference frame which is defined on the microgrid network ro-tating at angular frequency of ω. $d1$ -axis *and* $q1$ -axis, $d2$ -axis and $q2$ -axis, d -axis and q -axis are the local reference frames of DG1, DG2 and ESS rotating at ω, ω and ω, respectively.

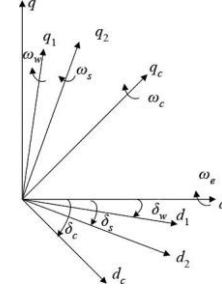Fig. 2. Global and local rotating reference frames of the microgrid.

$\delta_n (n = wsc)$ denotes the angle between the local reference frame of $d_n\_q_n (n = 12c)$ and the global reference frame, respectively:

$$\begin{bmatrix} \Delta f_{qn} \\ \Delta f_{dn} \end{bmatrix} = [T] \begin{bmatrix} \Delta f_q^g \\ \Delta f_d^g \end{bmatrix} + \begin{bmatrix} f_{dn} \\ f_{qn} \end{bmatrix} \Delta \delta_n$$
$$T = \begin{bmatrix} \cos \delta_n & -\sin \delta_n \\ \sin \delta_n & \cos \delta_n \end{bmatrix}. \tag{1}$$

In (1), $[f_n f_{dq}]_T$ is defi ned as the vector of f, which repre-sents the voltage or current component in the nth local reference frame. $[f_q f_d]_T$ is the vector of f in global reference frame, and $[f_{dn} f_c]_T$ is the steady-state value of f in the nth local refer-ence frame.

A. Mathematic Model of DG1

DG1 is mainly composed of wind turbine, transmission system, asynchronous generator and pitch control system. The electrical system of the three-phase symmetrical asynchronous generator in its arbitrary reference frame of $d1\_q1$ is given by

$$V^w = E I^w + F \frac{d}{dt}(I^w) \tag{2}$$

where

$$V^w = [V_{sq1}\ V_{sd1}\ V_{rq1}\ V_{rd1}]^T$$
$$I^w = [i_{sq1}\ i_{sd1}\ i_{rq1}\ i_{rd1}]^T$$

are the voltage and current vectors of the stator windings ($s1$s $d1$ and the rotor windings $rq1 rd1$, respectively, and matrices E and F can be derived in [13].

The rotor mechanical model of DG1 is represented as

$$\frac{d\omega_r}{\omega_b dt} = \frac{1}{2H}(T_e - T) \tag{3}$$

where ω_b and ω are the base electrical angular velocity and

the rotor electrical angular velocity, respectively. H is the combined inertia constant of rotor and loads. T is the mechanical torque, and T is the electromagnetic torque given by $_e$

$$ \underline{\quad} \underline{\quad} \underline{\quad\quad\quad\quad} \underline{\quad} \underline{\quad\quad\quad} \tag{4}$$

where $\blacksquare$ is the mutual inductance between stator and rotor windings.

The characteristics of wind turbine are stated as

$$\begin{cases} \lambda = R\,\dfrac{\omega_{wind}}{} \end{cases} \tag{5}$$

where λ is the ratio of rotor blade tip speed to wind speed. R_c is the turbine swept radius. ω_{wind} is the angular velocity of the wind turbine. V_{wind} is wind speed. T_W is the mechanical output torque of wind turbine. ρ is air density. C_T is the torque coeffi-cient. β is the blade pitch angle [14].

Wind turbine is connected to the asynchronous generator through a coaxial shaft where the mechanical model can be regarded approximately as a first-order time-delay system due to its large physical inertia, as shown in (6):

$$\frac{dT}{dt} = \frac{1}{T_H}(T_w \quad T) \tag{6}$$

where T_H is the inertia time constant.

The concept of slip s is defined in synchronous rotating ref-erence frame by setting $\omega = \omega$:

$$S = \frac{\omega_e - \omega_r}{\omega_e} \tag{7}$$

where ω_e is the synchronous electrical angular velocity. Then the model in synchronous rotating reference frame of d_q_1 is transformed into the global reference frame by (1).

The mathematical model of DG1 can be set up by (2)–(7). The small- signal state space model of DG1 in the global reference frame is

$$\Delta \dot{x}^{ws} = A_w \blacktriangle x^{ws} + B_v^w \blacktriangle n^w + B_u^w \blacktriangle n^w \tag{8}$$

$$\Delta x^{ws} = [\blacktriangle i_{sq1}^q\ \blacktriangle i_{sd1}^q\ \blacktriangle i_{rq1}\ \blacktriangle i_{rd1}\ \blacktriangle \omega_r\ \blacktriangle T]^T$$
$$\Delta v^w = [\blacktriangle V_{sq1}^q\ \blacktriangle V_{sd1}^q]^T$$
$$\Delta u^w = [\blacktriangle V_{rq1}\ \blacktriangle V_{rd1}\ \blacktriangle V_w]^T$$
$$\Delta V_w = \frac{\pi \rho C_T R_c^3 V_{wind}^\bullet}{T_H}\blacktriangle V_{wind}.$$

B. Mathematic Model of DG2

DG2 consists of a prime mover such as diesel engine and gas turbine, and a three-phase synchronous generator with excita-tion and governor control systems. The electrical system of the synchronous generator in rotor reference frame $d_2\_q_2$ is

$$V^s = GI^s + H\frac{}{dt}(I^s) \tag{9}$$

where

$$V^s = [V_{q2}\ V_{d2}\ V_{k1q2}\ V_{k2q2}\ V_{kd2}\ V_{fd2}]^T$$
$$I^s = [i_{q2}\ i_{d2}\ i_{k1q2}\ i_{k2q2}\ i_{kd2}\ i_{fd2}]^T$$

are the voltage and current vectors of the stator windings $(q2, d2)$, the damper windings $(k1q2, k2q2, kd2)$ and the field winding $(fd2)$, respectively. The matrices G and H can be derived from the methods shown in [13].

The mechanical model of the rotor of DG2 is given by

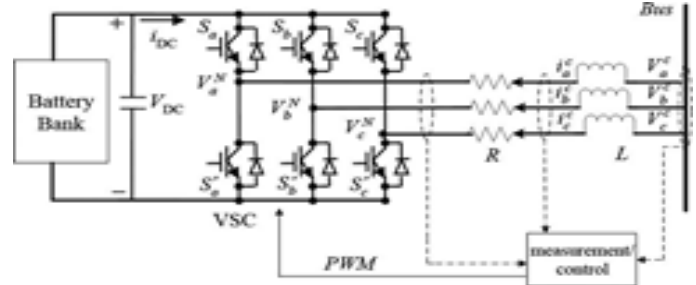$$\frac{d\omega}{} \quad 1 \tag{10}$$

Fig. 3. Schematic diagram of ESS

where ω is the rotor electrical angular velocity. H_s is the com-bined inertia constant of rotor and loads. T_M is the mechanical torque. T_{es} is the electromagnetic torque given by

$$T_{es} = X_{md}(-i_{d2} + i_{fd2} + i_{kd2})i_{q2}$$
$$-X_{mq}(-i_{q2} + i_{k1q2} + i_{k2q2})i_{d2} \tag{11}$$

where X_{md} and X_{mq} are the magnetizing inductances.

The mathematical model of DG2 can be established by (9)–(11), and transformed to the global reference frame pro-vided that the synchronous generator operates at the grid-con-nected mode. It is convenient to linearize the state equations in the synchronous rotating reference frame with the relationship of $\_$ and $\blacksquare$ given by

$$\frac{d\dot{\delta}_s}{dt} = \frac{\omega - \omega_e}{} .(12) \text{ Where } \omega_b \omega_b$$

Combined (12) with (1), the small-signal model of DG2 in the global reference frame are

$$\Delta \dot{x}^{ss} = A_s \blacktriangle x^{ss} + B_v^s \blacktriangle v^s + B_u^s \blacktriangle u^s \tag{13}$$

Where

$$\Delta x^{ss} = [\blacktriangle i_{q2}^q\ \blacktriangle i_{d2}^q\ \blacktriangle i_{k1q2}\ \blacktriangle i_{k2q2}\ \blacktriangle i_{kd2}\ \blacktriangle i_{fd2}\ \blacktriangle \dot{\delta}_s\ \blacktriangle \delta_s]^T$$
$$\Delta v^s = [\blacktriangle V_{q2}^q\ \blacktriangle V_{d2}^q]^T$$
$$\Delta u^s = [\blacktriangle V_{fd2}\ \blacktriangle T_M]^T.$$

C. Mathematic Model of ESS

Fig. 3 illustrates the schematic diagram of ESS, which consist of battery bank and power electronic circuit with corresponding control system, and filters. The filters can be equivalent as the series connection of a resistor (R) and an inductance (L) for each phase where R denotes the lump resistor of power line and converter, and the effect of the dead-time of IGBT bridges. V_{DC} is the DC -bus voltage and can be considered constant usually for dynamic analysis, which explains the concept of VSC.

In the local reference frame of d_q , the power circuit equations is given by

$$(14) \begin{bmatrix} \frac{di_{dc}}{dt} \\ \frac{di_{qc}}{dt} \end{bmatrix} = \begin{bmatrix} -\frac{R}{L} & \omega_b \\ -\omega_b & -\frac{R}{L} \end{bmatrix} \begin{bmatrix} i_{dc} \\ i_{qc} \end{bmatrix} + \frac{1}{L} \begin{bmatrix} V_{dc} - V_{dc}^N \\ V_{qc} - V_{qc}^N \end{bmatrix}$$

where V_N and V_N are the voltage components of VSC in dc_qc axis frame. V_{dc} and V_c are the voltage components
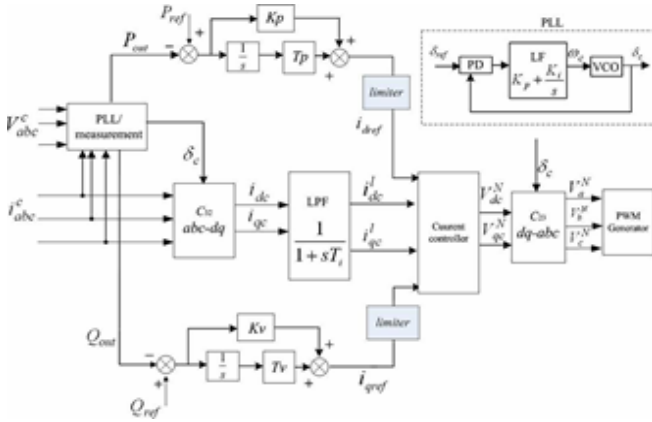

Fig. 4. External active/reactive power controller.

of AC-bus in dc_qc axis frame. i_{dc} and i_c are the current components of VSC in dc_qc axis, respectively.

Based on (14), the small-signal model of the power circuit of ESS is represented by

$$\Delta \dot{x}^{cs} = A_c \Delta x^{cs} + B_v^c \Delta v^c + B_u^c \Delta u^c + B_u^{\delta} \Delta \delta_c \quad (15)$$

Where

$$\Delta x^{cs} = [\Delta i_{qc}^s \; \Delta i_{dc}^s]^T$$
$$\Delta v^c = [\Delta V_{qc}^s \; \Delta V_{dc}^s]^T$$
$$\Delta u^c = [\Delta V_q' \; \Delta V_d']^T$$
$$V_q' = V_{qc} - V_{qc}^N - i_{dc}\omega_b L$$
$$V_d' = V_{dc} - V_{dc}^N + i_{qc}\omega_b L.$$

In the global reference frame, $\Delta \delta_c$ can be derived from [12].

A novel control strategy is put forward to control the VSC of ESS. It is composed of three controllers including external active/reactive power controller, inner current decoupling controller, and voltage feed-forward controller. The power controller generates the reference currents for the inner current controller according to the power requirements locally or remotely. The inner current controller and voltage feed-forward controller then generate the reference voltages(V_{dc}^N and V_{qc}^N) for VSC.

As shown in Fig. 4, the phase lock loop (PLL) is used to recognize the instantaneous phase of the electric network. The mathematical model of the PLL is represented by

$$\Delta \omega_c = \Delta \dot{\delta}_c (K_p + \frac{K_i}{s}) = K_p \Delta \omega \quad K_i \Delta \delta_c \quad (16)$$

where K_p, K_i are the PI coefficients of the PLL controller.

The small-signal model of the control system of ESS in the global reference frame is given by

$$\Delta \dot{x}^{cc} = A_{cc} \Delta x^{cc} + B_{cc} \Delta x^{cs} + B_v^{cc} \Delta v^c + B_u^{cc} \Delta u^{cc} \quad (17)$$

Where

$$\begin{bmatrix} \Delta f_{qn} \\ \Delta f_{dn} \end{bmatrix} = [T] \begin{bmatrix} \Delta f_q^g \\ \Delta f_d^g \end{bmatrix} + \begin{bmatrix} -f_{dn}^o \\ f_{qn}^o \end{bmatrix} \Delta \delta_n$$
$$T = \begin{bmatrix} \cos \delta_n & -\sin \delta_n \\ \sin \delta_n & \cos \delta_n \end{bmatrix}.$$

and ___ are the states of PI regulator of the current controller in ___ axis. ___ and ___ are the active and reactive power output of ESS. ___ and ___ are the filtered values of ___ an d ___. ___ and ___ are the filtered values of ___ and ___ an d respectively.

, (15)

Based on the relationship between ___ and ___ ___ can be rewritten as

$$\Delta \dot{x}^{cs} = A_c \Delta x^{cs} + B_v^c \Delta v^c + B_u^{cc} \Delta x^{cc} + B_u \Delta u^{cc}. \quad (18)$$

D. Mathematic Model of Network

As shown in Fig. 1, the model of network in abc, stationary reference frame is represented by

$$R_1 i^{l1} + \frac{L_1 d i^{l1}}{dt} = v^{PCC} - v^w$$
$$R_2 i^{l2} + \frac{L_2 d i^{l2}}{dt} = v^s - v^{PCC}$$
$$R_3 i^{l1} + \frac{L_3 d i^{l3}}{dt} = v^{PCC} - v^c$$
$$C_p \frac{d V^{PCC}}{dt} = i^{l2} \quad i^{l1} \quad i^{l3} \quad i^{l4} \quad (19)$$

where R_n and L_n are the line impedance of the n th branch i^{ln} is the nth branch current. v^{PCC}, v^w, v^s and v^c are the voltage vectors of PCC, *Bus-1*, *Bus-2* and *Bus-3*, respectively C_p is the equivalent capacitor of the loads, and

$$R_5(i^s - i^{l2}) + \frac{L_5 d(i^s \quad i^{l2})}{dt} = v^s \quad (20)$$

where i^s is the current vector of DG2.

The small-signal model of the power network of the micro-grid system in the global reference frame is represented by

$$\Delta \dot{x}_{net} = A_{net} \Delta x_{net} + B_{net}^w \Delta v^w + B_{net}^s \Delta v^s + B_{net}^c \Delta v^c \quad (21)$$

and

$$\Delta v^s = D_{net} \Delta x_{net} + D_{net}^n \Delta \dot{x}_{net} + D_{net}^s \Delta x^{ss} + D_{net}^{ns} \Delta \dot{x}^{ss} \quad (22)$$

where we can see the equation of Δx_{net} at the bottom of the page.

E. System Model

Based on the above subsystem models of DG1, DG2, ESS and network, the small-signal model of a multi -DG microgrid system can be obtained. Fig. 6 describes the block diagram

$$\Delta x_{net} = [\Delta i_q^{l1} \; \Delta i_d^{l1} \; \Delta i_q^{l2} \; \Delta i_d^{l2} \; \Delta i_q^{l3} \; \Delta i_d^{l3} \; \Delta i_q^{l4} \; \Delta i_d^{l4} \; \Delta v_q^{PCC} \; \Delta v_d^{PCC}]^T$$
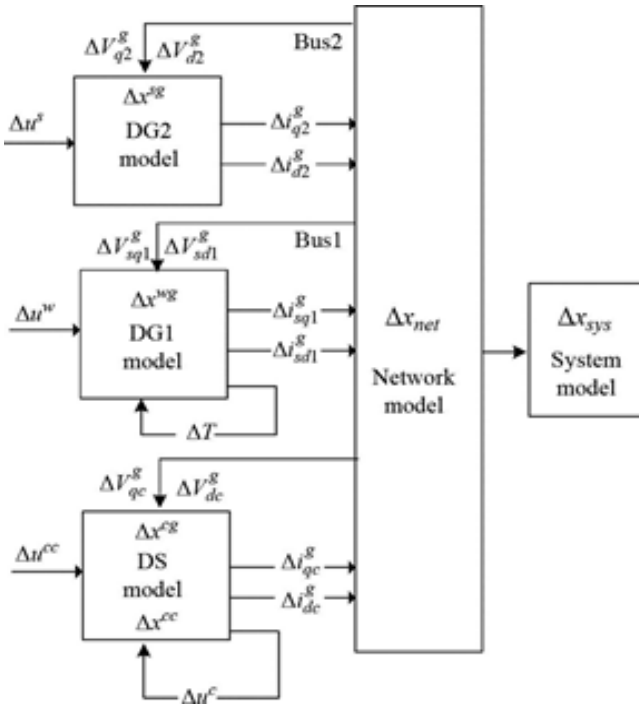
Fig. 5. Inner current controller.
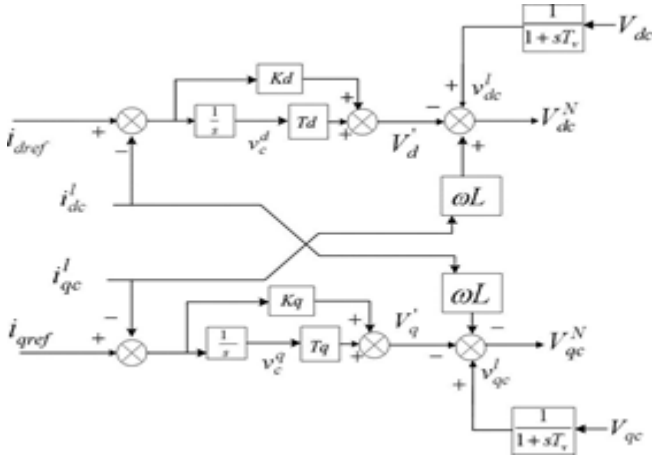
Elements	Type	Value
DG1	Rotor type	15 kVA
DG2	Rotor type	31.3 kVA
ESS	Inverter type	16 kVA
Line 1	Series RL Branch	$0.05128+j0.008\ (\Omega)$
Line 2	Series RL Branch	$0.04487+j0.007\ (\Omega)$
Line 3	Series RL Branch	$0.01282+j0.002\ (\Omega)$
Load1	Series RL Load	22.25 kW/18 kvar
Load2	Series RL Load	9.5 kW/1.2 kvar
Q_{cp}	Capacitor group	6 kvar

Fig. 6. Block diagram of the global small-signal model of a multi-DG micro-grid system.

TABLE II
EIGENVALUES OF THE STUDY MICROGRID SYSTEM

Eigen values	Real (1/sec)	Im (rad/sec)	Eigen values	Real (1/sec)	Im (rad/sec)
1, 2	-993.50	±38820	24	-10000	0
3, 4	-993.48	±38192	25	-10000	0
5, 6	-98.417	±340.89	26	-10000	0
7, 8	-2497.7	±314	27	-9997.5	0
9, 10	-1992.8	±314	28	-9997.3	0
11, 12	-393.32	±314	29	-106.97	0
13, 14	-161.18	±105.51	30	-60	0
15, 16	-6.57	±83.250	31	-50.831	0
17, 18	-63.241	±60.15	32	-24.409	0
19, 20	-1.3834	±10.357	33	-12.695	0
21, 22	-1.2636	±9.9276	34	-2.4	0
23	-10000	0	35	-0.41829	0

for developing state-space equations with all of the subsystem models integrated together. The node voltages (outputs of network) are taken as the input variables to the corresponding subsystems, and the node currents (outputs of subsystem) are taken as the output variables to the network.

The complete small-signal model and system state matrix (as given in (23)) can be obtained using the subsystem models de-noted by (8), (13), (17), (18), (21), and (22):

$$D_{sys}\blacktriangle\dot{x}_{sys} = A_{sys}\blacktriangle x_{sys} + B_{sys}\blacktriangle v_{sys} + C_{sys}\blacktriangle u_{sys} \quad (23)$$

where

$$\Delta x_{sys} = [\blacktriangle x^{wg}\ \blacktriangle x^{sg}\ \blacktriangle x^{cg}\ \blacktriangle x^{cc}\ \blacktriangle x_{net}]^T$$
$$\Delta v_{sys} = [\blacktriangle v^w\ \blacktriangle v^c]^T$$
$$\Delta u_{sys} = [\blacktriangle u^w\ \blacktriangle u^s\ \blacktriangle u^{cc}]^T.$$

III. DYNAMIC STABILITY ANALYSIS OF MICROGRID

The small-signal model can be used for eigenvalues anal-ysis to investigate the dynamic stability of microgrid system [15]–[18]. System stability margin and corresponding operation strategies can be obtained by tracking the loci of the eigenvalues with the variation of system parameters or steady-state oper-ating state.

A. Eigen Analysis

The proposed microgrid system shown in Fig. 1 is taken as an example with the main parameters listed in Table I.
Table II shows the eigenvalues of the microgrid study system under autonomous operation mode calculated by the linearized state matrix formulated by (23). There are 35 eigenvalues with all of the real parts being negative. Eigenvalues 1 to 22 are eleven pairs of complex-conjugate eigenvalues which represent eleven oscillatory modes. Eigenvalues (5, 6) and (17, 18) rep-resent the active and reactive power support by DG2 respec-tively corresponding to the electromagnetical interactions be-tween DG2 and the network. Eigenvalues (13, 14) and (15, 16) represent the active and reactive power supplied by DG1 re-spectively corresponding to the electromagnetical interactions between DG1 and the network. Eigenvalues (19, 20) and (21, 22) represent the reactive and active power support by ESS re-spectively corresponding to the electromagnetical

interactions between ESS and the network. The other five oscillatory modes represent the electromagnetical interactions among the network. The oscillation frequency and the damping of them depend on given operation conditions.

B. Sensitivity Analysis

Sensitivity analysis of system eigenvalues can be used to in-vestigate the dynamic stability margin of microgrid. It is con-ducted with respect to changes in various operation conditions.
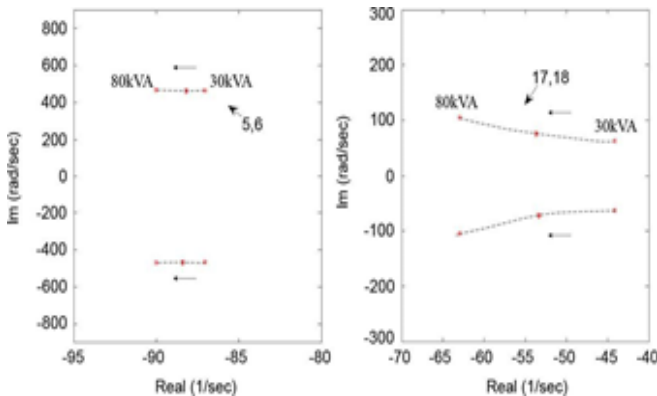

Fig. 7. Loci of eigenvalues (5, 6) and (17, 18) when the capacity of DG2 is changed from 30 kVA to 80 kVA.

Fig. 7 shows the loci of eigenvalues (5, 6) and (17, 18) where the capacity of DG2 is changed in condition that ESS is not equipped and the other system parameters shown in Table I are not changed. It reveals that the capacity increase of DG2 from 30 kVA to 80 kVA lead to the departure of the conjugate pairs of eigenvalues (5, 6) and (17, 18) from the right-hand plane to the left- hand plane, which increases the damping of the two modes and system stability margin is improved.

The characteristics analysis of DG2 reveals that the active and reactive power output of DG2 increase with its capacity, which result in the enhancement of system active/reactive power sup-port capacity. This is consistent with the trend of eigenvalues (5, 6) and (17, 18) based on sensitivity analysis.
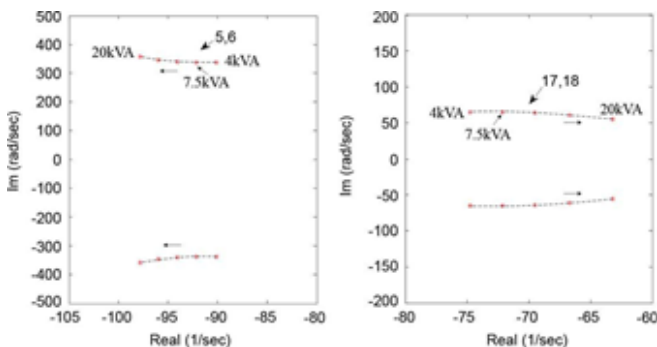

Fig. 8. Loci of eigenvalues (5, 6) and (17, 18) when the capacity of DG1 is changed from 4 kVA to 20 kVA.

Fig. 8 shows the loci of eigenvalues (5, 6) and (17, 18) when the capacity of DG1 is varied in condition that ESS is not equipped and the wind speed is steady at 10 m/s. It can be seen that with the capacity of DG1 increasing from 4 kVA to 20 kVA, eigenvalues (5, 6) move to the left -hand plane, which means the damping enhancement of the mode and

system stability margin improvement. However, eigenvalues (17, 18) move to the right-hand plane, resulting the damping decrease of the mode and system stability deterioration.

The sensitivity analysis of DG1 reveals that the active power output of DG1 rises with the increase of its capacity under the same wind speed status, meanwhile the reactive power absorp-tion of DG1 increase too. It results in the fact that system active power support capability is enhanced, whereas reactive power support capability is weakened. This restricts the install capacity of renewable energies.

Wind speed variation and disturbance will cause the output power fluctuations of DG1, which may affect the stability of microgrid. Fig. 9 depicts the loci of eigenvalues (5, 6), (13, 14),
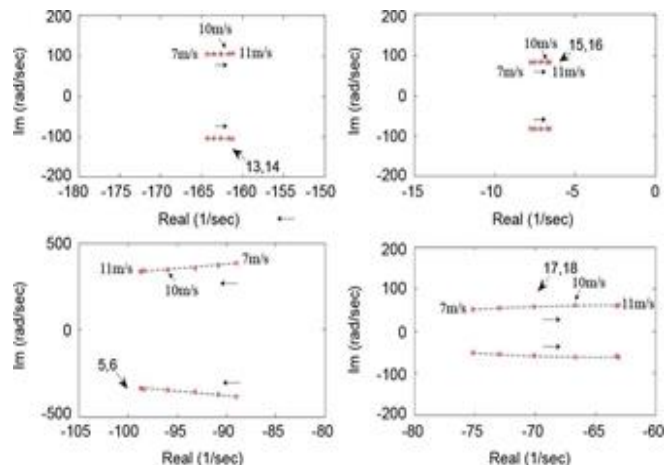

Fig. 9. Loci of eigenvalues (5, 6), (13, 14), (15, 16) and (17, 18) when wind disturbance occurs with the same DG1 capacity.

(15, 16) and (17, 18) with wind speed variation in the conditions that the capacity of DG1 remain unchanged and there is no ESS equipped. It indicates that the increasing of wind speed from 7 m/s to 11 m/s result in the departure of eigenvalues (13, 14) and (15, 16) to the right-hand plane, which will reduce the damping of the mode and then system dynamic stability.

It can also be seen from Fig. 9 that the increase of wind speed results in the departure of eigenvalues (5, 6) to the left-hand plane and eigenvalues (17, 18) to the right-hand plane. Ac-cording to the characteristics of squirrel asynchronous generator of DG1, the active power output increases with the wind speed, while the reactive power absorption of DG1 also increases. This results in that system active power support capacity is enhanced, whereas the reactive power support capacity is weakened. This means that microgrid dynamic stability differs with the wind conditions.

The impact of the output power fluctuating of DG1 on micro-grid can be mitigated or eliminated through the equipment of ESS. With proper control of power converter between battery bank and the microgrid, ESS can operate flexibly, absorbing/re-leasing energy quickly to maintain the instantaneous power bal-ance of the system. As a result, the stability is improved greatly.

Fig. 10 shows the loci of eigenvalues (5, 6) and (17, 18) when wind speed varies from 6 m/s to 11 m/s with ESS equipped in the study microgrid system. ESS is controlled to restrain system active power fluctuating, and to restrain system active/reactive
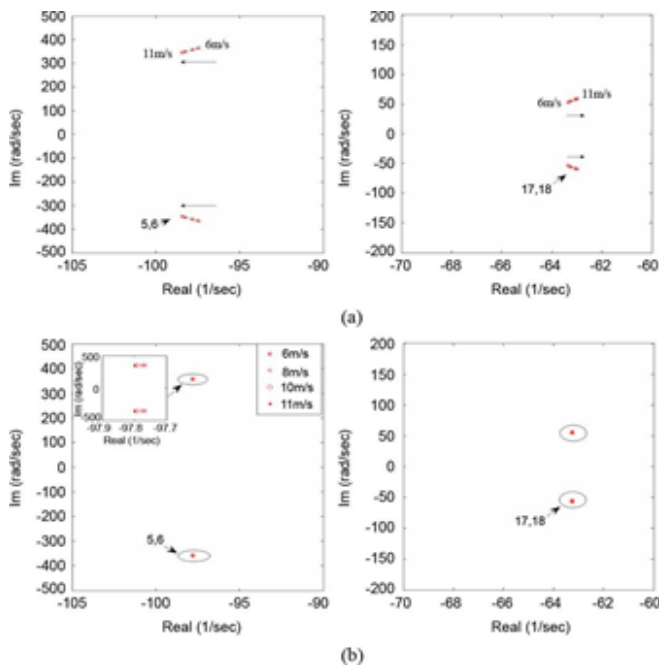
Fig. 10. Loci of eigenvalues (5, 6) and (17, 18) when wind
speed varies with ESS equipped. (a) ESS is controlled to
restrain active power fluctuation. (b) ESS is controlled to
restrain active/reactive power fluctuation.

power fluctuating, as shown in Fig. 10(a) and (b),
respectively. Compared with Fig. 9, the change of eigenvalues
loci of (5, 6) and (17, 18) in Fig. 10(a) under wind disturbance
can be re-strained greatly, while as shown in Fig. 10(b), they
are almost unaffected with wind disturbance. It reveals that
microgrid dy-namic stability can be improved with proper
control of ESS.

IV. SIMULATION AND EXPERIMENT RESULTS

A simulation platform of the study microgrid system shown
in Fig. 1 is established under MATLAB/SIMULINK
environ-ment. Table I shows the main parameters of the
system. The sim-ulation is implemented in time -domain to
test and verify system performance under wind gust
disturbance with/without energy storage.

The microgrid is controlled to operation in autonomous
mode. It stays originally in a steady operating state with wind
speed of 10 m/s. Then a wind gust occurs at $t=34.0$s. Fig. 11
shows the power output process of DG2 under the gust
disturbance with/without ESS, respectively.

As can be seen from Fig. 11(b), the gust disturbance lead to
DG2 active power fluctuating obviously with the fluctua-tion
ratio of 10% when ESS is not equipped. However, the ac-tive
power fluctuating is restrained largely with the fluctuation
ratio of around 1% and shortened recovery time when ESS is
used. Meanwhile, the wind gust disturbance lead to DG2
reac-tive power fluctuating with the fluctuation ratio of 12%
when ESS is not equipped, and decreased to 1.6% with ESS
used, as shown in Fig. 11(c).

The simulation results reveal the fact that ESS can release
or absorb power quickly and flexibly which track and
compensate the change of wind power precisely to mitigate
system instanta-neous power unbalance. ESS absorbs active
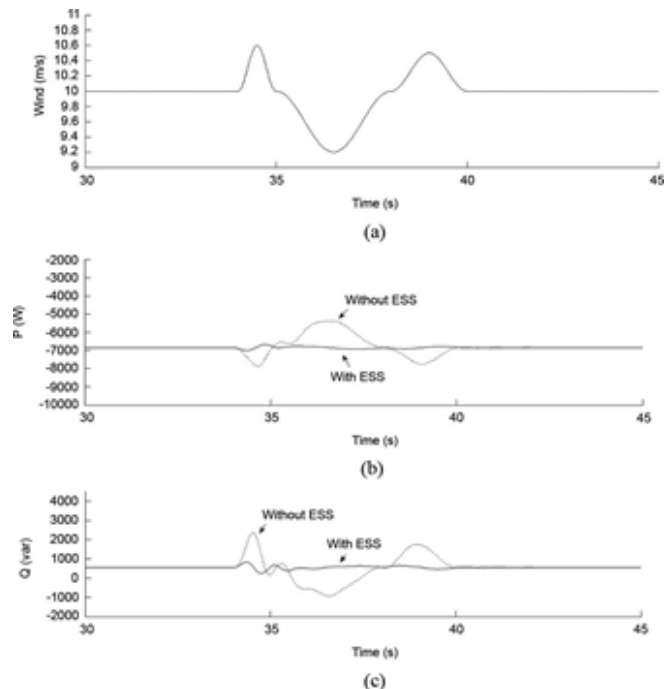
power and releases.

Fig. 11. System response to gust disturbance (with/without
ESS). (a) Wind speed. (b) Active power of DG2. (c) Reactive
power of DG2

reactive power when wind speed increases, and releases
active power and absorbs reactive power when wind speed
decreases. The amount of active/reactive power
released/absorbed by the ESS can be altered conveniently
through the control of the VSC between energy storage and
microgrid.

A microgrid experimental platform of the same configuration
and parameters as shown in Fig. 1 and Table I. is established in
the Microgrid Research and Test Laboratory of IEE, CAS.

Fig. 12 shows system response to wind gust disturbances
without ESS. The microgrid system is originally in autonomous
mode with 6 kW power output of DG1. Following the gust
oc-curs at $t=40.0$s, the output power of DG1 and DG2 change
accordingly, as shown in Fig. 12(a) and (b). The active power
output of DG2 decreases when that of DG1 increases with wind
speed to maintain global active power balance. Meanwhile, the
reactive power released from DG2 increases too to compensate
the rising of reactive power absorption of DG1. On the contrary,
when wind speed decreases, the active power output of DG1
decreases and that of DG2 increases. Meanwhile, the reactive
power output of DG2 decreases with the decline of the reactive
power absorption of DG1. The experiment results show that the
active/reactive power of DG2 fluctuates obviously during the
gust disturbance without ESS. This is not favorable for a thermal
engine since the frequently changing of operation state may
im-pose extra mechanical and electrical stress on the units.
Fig. 13 shows system response to gust disturbance with ESS.
As mentioned above, ESS can track the output power changes
of DG1 precisely and mitigate the adverse effects through
active/reactive power output/input of ESS quickly and
flexibly due to its decoupling controller. As a result, the
instantaneous power unbalance is mitigated and the frequency
and voltage quality and stability of the microgrid is improved
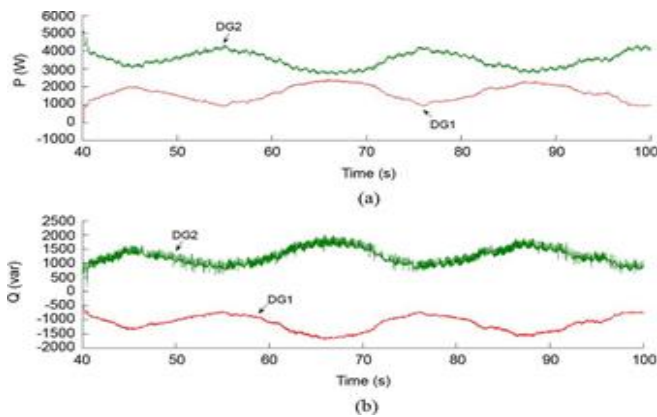
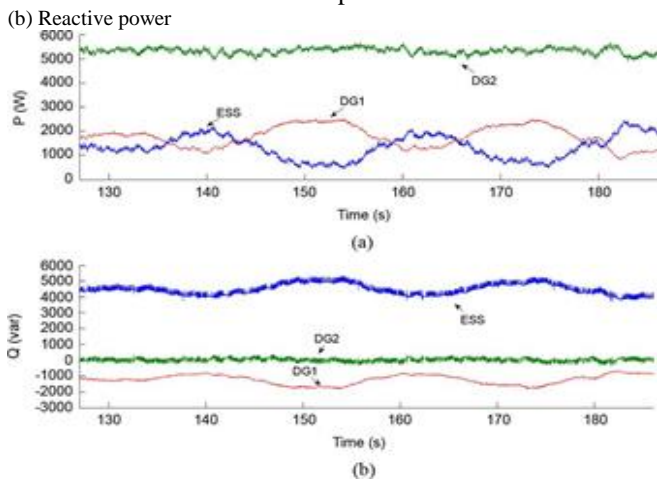Fig. 12. System response to gust disturbance without ESS. (a) Active power

(b) Reactive power

Fig. 13. System response to gust disturbance with ESS. (a) Active power.
(b) Reactive power

greatly. Specifi cally, ESS absorbs active power and releases reactive power when wind speed increases, whereas output active power and absorbs reactive power when wind speed decreases, as shown in Fig. 13(a) and (b). According to the experiment results, the active/reactive power of DG2 is main-tained stable during the gust disturbance with the help of ESS. Moreover, the thermal engine in a microgrid can be maintained at a high-efficient operating state and system fuel economic is improved.

V. CONCLUSION

In this paper, a comprehensive small-signal model of a typical microgrid is presented including synchronous generator, asyn-chronous generator, and voltage source converter with corre-sponding control systems. The model covers almost all the pos-sible power interfaces of DG and ESS existing in microgrid or distributed generation system. All the subsystems are modeled individually and then combined on a global reference frame. The model of different kind of microgrids can be obtained easily based on this paper with proper adjustment of the number and parameters of the subsystems.

The model is analyzed in terms of system eigenvalues and their sensitivity to different operating state and control strategies of DG or ESS. It is observed that the dynamic stability of an au-tonomous microgrid is influenced by system configuration and the variability of intermittent generation. It can be improved re-markably with ESS equipped due to its ability to mitigate the

in-stantaneous active/reactive power unbalance. Therefore, prop-erly designed and controlled energy storage is an essential solu-tion to the reliable operation of microgrid as well the effective utilization of renewable energy.

Results obtained from the model and eigenvalues analysis were verified through simulation and experiment on a study microgrid system. It can be observed that the model and its eigenvalues successfully denote the relationship between the dynamic stability and system configuration and the corre-sponding operation state.

This paper provides a theoretical foundation for the anal-ysis, confi guration and operation of microgrid especially in au-tonomous operation mode. It enables the design and control of microgrids to achieve the objective of both reliability of power system and effective utilization of renewable resources.

REFERENCES

[1] R. H. Lasseter, "Microgrids," in *Proc. IEEE Power Eng. Soc. Winter Meeting*, Jan. 2002, vol. 1, pp. 305–308.

[2] R. H. Lasseter, "Certs microgrid," in *Proc. IEEE Syst. of Syst. Eng. Conf.*, 2007, pp. 1–5.

[3] A. G. Tsikalakis and N. D. Hatziargyriou, "Centralized control for op-timizing microgrids operation," *IEEE Trans. Energy Convers.*, vol. 23, no. 1, pp. 241–248, Mar. 2008.

[4] H. Nikkhajoei and R. H. Lasseter, "Distributed generation interface to the CERTS microgrid," *IEEE Trans. Power Del.*, vol. 24, no. 3, pp. 1598–1608, Jul. 2009.

[5] F. Katiraei, M. R. Iravani, and P. W. Lehn, "Small-signal dynamic model of a microgrid including conventional and electronically inter-faced distributed resources," *IET Gener. Transm. Distrib.*, vol. 1, no. 3, pp. 369–378, May 2007.

[6] N. Pogaku, M. Prodanovic, and T. C. Green, "Modeling, analysis and testing of autonomous operation of an inverter-based microgrid," *IEEE Trans. Power Electron.*, vol. 22, no. 2, pp. 613–624, Mar. 2007.

[7] A. L. Dimeas and N. D. Hatziargyriou, "Operation of a multiagent system for microgrid control," *IEEE Trans. Power Syst.*, vol. 20, no. 3, pp. 1447–1455, Aug. 2005.

[8] J. A. P. Lopes, C. L. Moreira, and A. G. Madureira, "Defining control strategies for microgri ESS islanded operation," *IEEE Trans. Power Syst.*, vol. 21, no. 2, pp. 916–924, May 2006.

[9] D. J. Lee and L. Wang, "Small-signal stability analysis of an au-tonomous hybrid renewable energy power generation/energy storage system part I: time-domain simulations," *IEEE Trans. Energy Con-vers.*, vol. 23, no. 1, pp. 311–320, Mar. 2008.

[10] C. Abbey and G. Joos, "Supercapacitor energy storage for wind energy applications," *IEEE Trans. Ind. Appl.*, vol. 43, no. 3, pp. 769–776, May 2007.

[11] J. P. Barton and D. G. Infield, "Energy storage and its use with inter-mittent renewable energy," *IEEE Trans. Energy Convers.*, vol. 19, no. 2, pp. 441–448, Jun. 2004.

[12] F. Katiraei, "Dynamic analysis and control of distributed energy re-sources in a microgrid," Ph.D. dissertation, Univ. Toronto, Toronto, ON, Canada, 2005.

[13] P. C. Krause, *Analysis of Electric Machinery*. New York, NY, USA: McGraw-Hill, 1986.

[14] F. Blaabjerg, Z. Chen, and S. B. Kjaer, "Power electronics as efficient interface in dispersed power generation systems," *IEEE Trans. Power Electron.*, vol. 19, no. 5, pp. 1184–1194, Sep. 2004.

[15] E. A. A. Coelho, P. Cortizo, and P. F. D. Gracia, "Small signal sta-bility for parallel-connected inverters in stand-alone ac supply sys-tems," *IEEE Trans. Ind. Appl.*, vol. 38, no. 2, pp. 533–542, Mar. 2002.

[16] F. Katiraei and M. R. Iravani, "Power management strategies for a mi-crogrid with multiple distributed generation units," *IEEE Trans. Power Syst.*, vol. 21, no. 4, pp. 1821–1831, Nov. 2006.

[17] P. Kundur, *Power System Stability and Control*. New York, NY, USA: EPRI/McGraw-Hill, 1994.

[18] K. Ogata, *Modern Control Engineering*. Englewood Cliffs, NJ, USA: Prentice Hall, 2001.